Itinerant to localized electronic behavior in phase segregated ruthenates

CrossMark

Biswajit Dalal, Babusona Sarkar, S.K. De[*]

Department of Materials Science, Indian Association for the Cultivation of Science, Jadavpur, Kolkata 700032, India

A B S T R A C T

Simultaneous doping of Ba and Zr for Sr and Ru in $SrRuO_3$ leads to phase separation of orthorhombic $SrRuO_3$ (SRO) and nine layer rhombohedral $BaRuO_3$ (9R-BRO). Differences in ionic radius and electronegativity between the cations are responsible for the chemical phase separation with increase of doping concentration. Random substitution of Ru by Zr localizes electron and induces Metal-Insulator (M–I) transition for lower doping concentration (5% and 10%). Electron–electron interaction dominates electrical conduction process due to cationic disorder in SRO lattice. Dilution of ferromagnetic interaction due to non-magnetic element Zr decreases both Curie temperature and Curie-Wiess constant and produces Griffiths phase just above the Curie temperature. At higher doping concentration (40%), solid solution of ruthenates reveals magnetism purely related to 9R-BRO phase.

© 2016 Elsevier B.V. All rights reserved.

1. Introduction

Ruddlesden-Popper (RP) series of ruthenates $Sr_{n+1} Ru_nO_{3n+1}$, where n is the number of RuO_6 octahedra layers within the unit cell, have drawn much interest to the researchers due to its exotic electronic and magnetic properties, depending on the number of RuO_6 octahedra layers in the unit cell [1–3]. $SrRuO_3$ (SRO) (with $n = \infty$) is one of the most promising and fascinating material in this series, not only because of itinerant ferromagnetic properties with highest Curie temperature ($T_C = 160-165$ K) [4], but also due to its potential application as conductive electrode in spintronic devices [5] and magnetic tunnel junctions [6]. SRO also exhibits metallic property, like all other n in this RP series. Non-Fermi-liquid like behavior, non-saturating behavior of resistivity (when passing through the Ioffe-Regel limit) and linear relationship of resistivity with temperature at high temperature defines SRO as "bad metal" [7–9]. Room temperature resistivity of 4d-based oxide SRO ($\rho_{RT} \sim 10^{-4}$ Ω-cm) is also two orders of magnitude higher than the conventional good metallic ferromagnet like iron, nickel and cobalt ($\rho_{RT} \sim 10^{-6}$ Ω-cm) [10]. Relatively high density of state (DOS) at the Fermi level (E_F) and delocalized Ru 4d orbital are responsible for the itinerant ferromagnetic ground state of SRO [11]. Band structure calculation suggests the collective band magnetism in SRO, rather

than atomic and also explains the reduced ferromagnetic moment (varies between 0.8 μ_B/Ru and 1.6 μ_B/Ru) far below Curie temperature (T_C), which is less than the low-spin (S = 1) state of Ru^{4+} ion [12].

Larger hybridization between Ru 4d and O 2p orbitals, due to extended 4d-shell of Ru, gives rise to greater itinerancy of electrons in SRO as compared to 3d transition-metal oxides and plays an important role in determining the physical properties of perovskite ruthenates [13,14]. Local-density approximation (LDA) based band theory predicts that minority spin electrons are responsible for most of transport currents in ferromagnetic phase, due to shorter mean free path (smaller Fermi velocity) of majority spin electron [12]. Experimental investigation on transport properties suggests that the room temperature mean free path is about 10 Å for conduction electron in SRO [12]. Impurity doping strongly affects on lattice distortion and p-d hybridization of SRO, which in turn modifies characteristic behavior such as itinerant or localized nature of conduction electron and consequently its mean free path. Generally, impurity doping leads to lattice disorder in SRO and destroys itinerant properties of electron [15]. Divalent Ca substitution at Sr-site of SRO, does not affect much more the metallic properties but destroys ferromagnetism [14]. On the other hand, larger ionic Ba^{2+} substitution, decreases the T_C by band broadening [16]. Gradual loss of ferromagnetism and metal to insulator (M–I) transition with increasing doping concentration have been found in larger cations (La and K) co-substituted SRO [17], which opposes the theoretical calculation by Mazin *et al* [11]. Subtle percentage of

* Corresponding author.
  E-mail address: msskd@iacs.res.in (S.K. De).

non-magnetic impurity substitution at Ru-site causes electron localization and drives the sample into M−I transition state [18]. Increasing tendency of ferromagnetic Curie temperature (T_C) has been observed for Cr-doped SRO, due to e_g^0 electronic configuration of Cr^{3+} (high spin) [19]. Dilution of ferromagnetic phase with impurity substitution also leads to rich magnetic phases like spin glass, cluster glass, antiferromagnetism and Griffiths phase [16,20–22].

In most of impurity substituted SRO either at Sr or Ru site reveals the evolution of single phase with the composition. However, cationic size mismatch and charge imbalance between particular site of a crystal and dopant ion, does not allow dopant ion for complete solid-solution throughout the whole compositional range and gives rise to mixed crystalline phases. In literature, fewer studies have been reported on physical properties of phase segregated SRO induced by dopants. Previously, it was reported that, complete solid-solution (with single phase) exists in $SrTi_{1-x} Ru_xO_3$ system [23,24]. Recently Jang et al by high-resolution synchrotron X-ray diffraction measurement have predicted that complete solid-solution exists only for a certain concentration region (20%) of Ti [25]. Higher concentration of Ti leads to the formation of $SrTiO_3$ and SRO instead of single phase. The spontaneous phase separation of hexagonal $BaTiO_3$ and orthorhombic SRO also has been observed in isovalent Ba and Ti co-doped SRO for higher doping concentration [26]. Replacement of Sr and Ru by isovalent non-magnetic Ba and Zr in SRO, may be one of the possible way by chemical substitution to tune the ferromagnetic and metallic properties of SRO. Formation of mixed phase like, $BaZrO_3$ (BZO) and $BaRuO_3$ (BRO) may also lead to interesting electronic and magnetic properties of the as-studied system. BZO is a paraelectric insulator [27], whereas BRO possesses a rich crystalline, electronic (Metallic, Metal to Insulator transition depending on crystalline phases) and magnetic (Paramagnetic, Antiferromagnetic) phases [28,29]. In this paper, we report the effect of larger size cation Ba and Zr co-substitution on structural, transport and magnetic properties of SRO. Chemical phase segregation, Metal → single M−I transition → double M−I transition → semiconductor and loss of ferromagnetism are observed with increasing non-magnetic impurity concentration.

2. Experiment

Polycrystalline samples of pure $SrRuO_3$ and Ba and Zr co-doped samples of the system $Sr_{1-x} Ba_xRu_{1-x} Zr_xO_3$, where $x = 0.05$, 0.10, 0.15, 0.20, 0.30 and 0.40 were prepared using standard solid state reaction method. $SrCO_3$, $BaCO_3$, RuO_2 and ZrO_2 were used as starting raw materials. Stoichiometric ratio of starting raw materials were weighed and mixed in an agate mortar and ground for 1 h. The mixed powders were calcined at $600°$ C for 24 h. After room temperature cooling, the samples were reground thoroughly for better homogeneity of the samples and pressed into cylindrical pellets using uniaxial hydraulic press. These pellets were sintered at $1150°$ C for 24 h and were quenched to room temperature from $900°$ C for better crystalline phases. These sintering processes were repeated once more with intermediate grinding for better homogeneity and crystallinity.

Pure crystalline phases were identified by X-ray diffraction method using X-ray powder diffractometer (X-pert Pro, PANalytical) in the range $15°−80°$ using Cu K_α radiation ($\lambda = 1.54\,Å$). The detailed structural parameters were obtained with the help of Rietveld refinement of diffraction patterns using MAUD software [30]. Temperature dependent dc resistivity of sintered pellet samples with rectangular parallelepiped shape was measured by Physical Properties Measurement System (PPMS, Cryogenics Ltd., UK) using four-probe technique in the temperature range 4−300 K. DC magnetization measurements were performed by Quantum

design SQUID magnetometer (MPMS XL Evercool model) in the temperature range 2−300 K.

3. Results

3.1. Crystal structure

Pure $SrRuO_3$ (SRO) crystallizes in orthorhombic symmetry with space group *Pnma* and the crystal structure is refined according to JCPDS card No. 871241 (ICSD card No. 082979). Detailed structural analysis for all the compositions ($0 \leq x \leq 0.40$) confirms the single phase orthorhombic structure only for $x = 0$ and 0.05. A different chemical phase starts to segregate with increasing doping concentration ($x \geq 0.10$). Room temperature X-ray powder diffraction data for $x = 0.1$ and 0.2 are shown in Fig. 1. Characteristic peak positions of segregated chemical phase as indicated by asterisks in Fig. 1 ensure the second phase as nine layer rhombohedral 9R-$BaRuO_3$ (9R-BRO), rather than BZO and $SrZrO_3$ (SZO) phases. Reason behind the formation of 9R-BRO, apart from BZO and SZO, is discussed later. 9R-BRO is the most stable phase in open air synthesis (at ambient pressure) among five possible perovskite-related structure of $BaRuO_3$ [28,29]. 9R-BRO crystallizes in rhombohedral symmetry with space group $R\bar{3}m$. Structural refinements for phase segregated samples ($x \geq 0.10$) were done using orthorhombic structure of SRO and rhombohedral structure of 9R-BRO. During refinement of diffraction patterns we have considered a general formula $(1-x)SrRu_{1-x} Zr_xO_3 − xBaRu_{1-x} Zr_xO_3$ for phase separated compositions $x \geq 0.10$ to maintain the proper stoichiometric ratio. We have precisely refined the XRD data with Zr doped SRO and 9R-BRO rather than separate BZO phases. The reliability of refinement depends on the conventional residual R_p, weighted residual R_{wp} and goodness of fitting (GOF) which are shown in Fig. 1. All these values indicate the best fitted XRD patterns for all compositions.

Variation of lattice parameters with composition for SRO and 9R-BRO are shown in Fig. 2(a) and (b), respectively. Lattice parameters for both SRO and 9R-BRO increase with increasing x. Fig. 2(c) shows the variation of unit cell volume for SRO and 9R-BRO with compositions which gradually increases with dopant concentration. The ionic radii of Sr^{2+}, Ba^{2+}, Ru^{4+}, and Zr^{4+} are 1.44 Å,
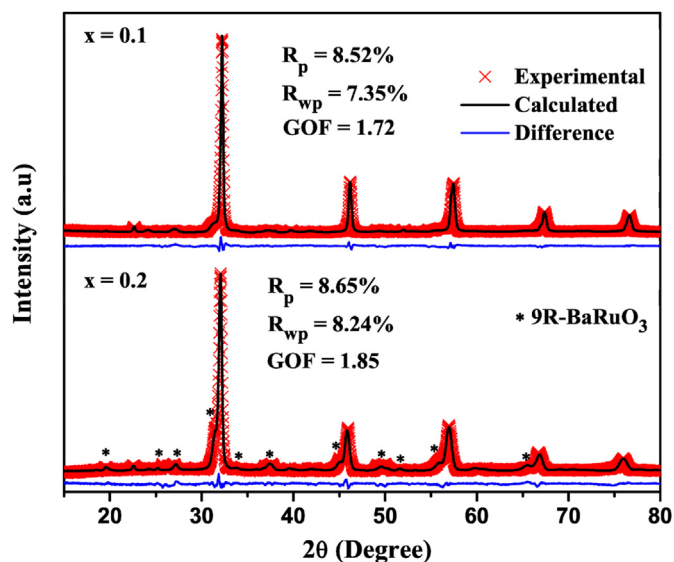

Fig. 1. Room temperature Rietveld fitted X-ray diffraction (XRD) patterns for $x = 0.10$ and 0.20. 9R-BRO phase is refined according to JCPDS card No. 711524 (ICSD card No.010253). 9R-BRO reflections are marked by the asterisks.